CORRIGENDUM

Development 137, 4327 (2010) doi:10.1242/dev.061747

RPK2 is an essential receptor-like kinase that transmits the CLV3 signal in *Arabidopsis*

Atsuko Kinoshita, Shigeyuki Betsuyaku, Yuriko Osakabe, Shinji Mizuno, Shingo Nagawa, Yvonne Stahl, Rüdiger Simon, Kazuko Yamaguchi-Shinozaki, Hiroo Fukuda and Shinichiro Sawa

A reference was omitted in *Development* **137**, 3911-3920.

In the first sentence on p. 3912, a paper by Jeong et al. (Jeong et al., 1999) should have been cited.

Reference

Jeong, S., Trotochaud, A. E. and Clark, S. E. (1999). The Arabidopsis CLAVATA2 gene encodes a receptor-like protein required for the stability of the CLAVATA1 receptor-like kinase. *Plant Cell* **11**, 1925-1933.

The authors apologise to readers for this mistake.

Development 137, 3911-3920 (2010) doi:10.1242/dev.048199

RPK2 is an essential receptor-like kinase that transmits the CLV3 signal in *Arabidopsis*

Atsuko Kinoshita[1], Shigeyuki Betsuyaku[1,2], Yuriko Osakabe[3], Shinji Mizuno[4,5], Shingo Nagawa[1,6], Yvonne Stahl[7], Rüdiger Simon[7], Kazuko Yamaguchi-Shinozaki[3,5], Hiroo Fukuda[1] and Shinichiro Sawa[1,*]

SUMMARY

The shoot apical meristem (SAM) is the fundamental structure that is located at the growing tip and gives rise to all aerial parts of plant tissues and organs, such as leaves, stems and flowers. In *Arabidopsis thaliana*, the CLAVATA3 (CLV3) pathway regulates the stem cell pool in the SAM, in which a small peptide ligand derived from CLV3 is perceived by two major receptor complexes, CLV1 and CLV2-CORYNE (CRN)/SUPPRESSOR OF LLP1 2 (SOL2), to restrict *WUSCHEL* (*WUS*) expression. In this study, we used the functional, synthetic CLV3 peptide (MCLV3) to isolate CLV3-insensitive mutants and revealed that a receptor-like kinase, RECEPTOR-LIKE PROTEIN KINASE 2 (RPK2), also known as TOADSTOOL 2 (TOAD2), is another key regulator of meristem maintenance. Mutations in the *RPK2* gene result in stem cell expansion and increased number of floral organs, as seen in the other *clv* mutants. These phenotypes are additive with both *clv1* and *clv2* mutations. Moreover, our biochemical analyses using *Nicotiana benthamiana* revealed that RPK2 forms homo-oligomers but does not associate with CLV1 or CLV2. These genetic and biochemical findings suggest that three major receptor complexes, RPK2 homomers, CLV1 homomers and CLV2-CRN/SOL2 heteromers, are likely to mediate three signalling pathways, mainly in parallel but with potential crosstalk, to regulate the SAM homeostasis.

KEY WORDS: *Arabidopsis*, Meristem, CLAVATA3 signalling pathway, Receptor-like kinase

INTRODUCTION

Multicellular organisms require the precise coordination of cell division and differentiation to ensure organised development. Plants have evolved a unique structure called the meristem, which consists of cells that divide continuously and renew themselves. Two major meristems, the shoot apical meristem (SAM) and the root apical meristem (RAM), are located on the top and the bottom ends of the apical-basal axis, respectively, and are responsible for providing cells for postembryonic growth and development. Each meristem forms repetitive structures, and is maintained throughout the life of the plant. In *Arabidopsis thaliana*, the SAM is divided into three areas: the peripheral zone (PZ), the central zone (CZ) and the rib zone (RZ). In the CZ, undifferentiated stem cell resides just above the organising centre (OC), and their descendant cells displaced to PZ are recruited into organ differentiation. The RAM, on the other hand, consists of several cell files, which originate from the stem cells surrounding the quiescent centre (QC) (Miwa et al., 2009a; Tucker and Laux, 2007).

[1]Department of Biological Sciences, Graduate School of Science, University of Tokyo, Hongo 7-3-1, Bunkyo-ku, Tokyo 113-0033, Japan. [2]Division of Life Sciences, Komaba Organization for Educational Excellence (KOMEX), Graduate School of Arts and Sciences, University of Tokyo, Komaba 3-8-1, Meguro-ku, Tokyo 153-8902, Japan. [3]Laboratory of Plant Molecular Physiology, Graduate School of Agricultural and Life Sciences, The University of Tokyo, Tokyo 113-8657, Japan. [4]Graduate School of Science and Technology, Chiba University, Inage, Chiba 263-8522, Japan. [5]Biological Resources Division, Japan International Research Center for Agricultural Sciences, Tsukuba, Ibaraki 305-8686, Japan. [6]Botany and Plant Sciences, University of California, Riverside, 3401 Watkins Drive, Riverside, CA 92521, USA. [7]Institut für Genetik der Heinrich-Heine Universität, D-40225 Düsseldorf, Germany.

*Author for correspondence (sawa@biol.s.u-tokyo.ac.jp)

Accepted 14 September 2010

Genetic studies have revealed that members of a homeobox gene family play a pivotal role in meristem maintenance. In the SAM, the WUSCHEL (WUS) homeodomain transcription factor is expressed in the OC and its activity promotes stem cell fate in a non-cell autonomous manner (Mayer et al., 1998). By contrast, a small signalling peptide encoded by *CLAVATA3* (*CLV3*) is secreted from stem cell to restrict *WUS* expression, thus establishing a negative feedback loop (Brand et al., 2000; Clark et al., 1995; Schoof et al., 2000). This *CLV3*-*WUS* negative feedback loop is represented by the opposite phenotype of these loss-of-function mutants: *wus* mutants exhibit SAM termination, whereas *clv3* mutants produce an enlarged SAM (Clark et al., 1995; Laux et al., 1996). This model is also supported by the fact that *CLV3* overexpression leads to *wus*-like phenotype (Brand et al., 2000). Recently, genetic and biochemical studies have demonstrated that the conserved C terminus of the CLV3 protein, the CLV3/ESR (CLE) domain, is necessary and sufficient for its function, and a series of exogenously applied synthetic peptides corresponding to the CLE domain is able to mimic the *CLV3* overexpression phenotype (Fiers et al., 2006; Fiers et al., 2005; Kondo et al., 2006; Sawa et al., 2008; Sawa et al., 2006). Although the *clv3* mutants develop normal roots, the synthetic CLV3 peptides, as well as *CLV3* overexpression induce RAM consumption in a *CLV2*-dependent manner, suggesting that there is a CLV-like pathway for sensing CLV3 ligand in roots (Clark et al., 1995; Fiers et al., 2005).

In the SAM, at least two receptor complexes function for the CLV3 recognition. *CLV1*, which encodes a member of leucine-rich repeat (LRR) receptor-like kinase (RLK), is expressed at the centre of the SAM, including the *WUS*-expressing OC, and the extracellular domain of the protein has been proved to bind CLV3 peptides (Clark et al., 1993; Ogawa et al., 2008; Ohyama et al.,

2009). In the second pathway, CLV2, an LRR receptor-like protein lacking a cytoplasmic domain, acts together with a membrane-associated protein kinase, CORYNE (CRN)/SUPPRESSOR OF LLP1 2 (SOL2), to transmit the CLV3 signal (Casamitjana-Martínez et al., 2003; Kayes and Clark, 1998; Miwa et al., 2008; Miwa, 2009b; Müller et al., 2008). The CRN/SOL2-CLV2 interaction is shown to promote the plasma membrane localization of the complex, where the complex is supposed to perceive extracellular CLE ligand signal(s). The homo-oligomer of CLV1 is able to weakly interact with CRN/SOL2-CLV2 complex, presumably via CRN/SOL2, suggesting a potential crosstalk between two CLV3 signalling pathways (Bleckmann et al., 2010; Zhu et al., 2009).

Nevertheless, these two complexes can independently transmit the CLV3 signal, because a *crn* mutation exerts an additive effect on the *clv1* phenotype. However, *clv1 crn* double mutants have slightly smaller inflorescence meristems and fewer carpels than single *clv3* mutants, suggesting the presence of an additional receptor complex that allows CLV3 signalling (Müller et al., 2008).

In this study, we showed that an LRR-RLK, RECEPTOR-LIKE PROTEIN KINASE 2 (RPK2), also known as TOADSTOOL 2 (TOAD2), is involved in maintenance of the SAM and the RAM downstream of a synthetic CLV3 peptide. A loss-of-function mutant of *RPK2* exhibited a *clv*-like phenotype, and is additive to both *clv1* and *clv2*. Furthermore, biochemical analysis using *Nicotiana benthamiana* demonstrated a biochemical interaction between CLV2-CRN/SOL2, but failed to detect an interaction between RPK2 and any of the other receptor proteins: CLV1, CLV2 and CRN/SOL2. These observations suggest that RPK2 is an essential component of an independent third pathway for CLV3 signalling.

MATERIALS AND METHODS

Plant materials and growth conditions

Arabidopsis wild-type and mutant lines were obtained as follows: Columbia-0 (Col-0), Wassilewskija-2 (Ws-2), *clv1-101* (CS858348) in Col-2 background, *clv3-8 ER* in unknown background (CS3604) (Diévart et al., 2003), *rpk2-1* in Col-0 background, *rpk2-2* in Col-0 background and *rpk2-3* (CS3960) in Ws-2 background (ABRC Stock Centre, Ohio, USA); *clv2-101* (GK686A09) in Col-0 background (GABI-kat, Bielefeld, Germany); *wus-101* (GK870H12) in Col-0 background (Prof. Jan Lohmann, University of Heidelberg, Heidelberg, Germany); *35S::RPK2* in Col-0 background (Prof. Kazuko Yamaguchi Shinozaki, University of Tokyo, Tokyo, Japan) (Mizuno et al., 2007).

For mature plant materials, seeds were sown on soil. For root and seedling assays, surface-sterilized seeds were plated on growth medium containing Murashige and Skoog basal salts, 1% (w/v) sucrose, 0.05% (w/v) MES (pH 5.7) and 1.5% (w/v) agar. Seeds were then transferred to a growth room at 22°C under continuous white light (20-50 mmol $m^{-2}s^{-1}$). MCLV3 was synthesized as described previously (Kondo et al., 2006).

Screening and map-based cloning of *cli1*

cli1/rpk2-4 was isolated from the ethylmethane-sulfonate (EMS)-mutagenized population generated previously (Sawa et al., 2005), and was backcrossed three times before further analyses. To map the *CLI1* locus, the *cli1* mutant in Columbia-0 (Col-0) background was crossed to Landsberg *erecta* (La-*er*) and homozygous mutants were selected in the F_2 population for segregation analyses. For their male sterility, all *rpk2* alleles were screened for their homozygosity using a PCR strategy.

Construction of transgenic plants

For the complementation test and expression analysis, the *RPK2*- and the *GFP*-coding region were combined using PCR with overlapping primers, and *Sma*I and *Bam*HI restriction sites were introduced at each end. The 1310 bp promoter and 983 bp terminator of *RPK2* were amplified by PCR, with *Sma*I and *Bam*HI sites, respectively. Each fragment was cloned into the gateway entry vector pENTR-D/TOPO in accordance with the manufacturer's instructions (Invitrogen, Carlsbad, CA, USA), and fused using corresponding restriction enzymes (TaKaRa, Shiga, Japan) and Ligation High enzyme (TOYOBO, Osaka, Japan). The entry vector possessing the full *pRPK2::RPK2-GFP:ter* fragment was verified by sequencing, and subsequently transferred to the gateway-compatible binary vector pGWB1 using LR clonase (Invitrogen). For the *35S::WUS* construct, *WUS*-coding region was amplified from reverse-transcribed total RNA of wild-type inflorescence meristem, and was cloned into pENTR-D/TOPO, subsequently transferred to the gateway-compatible binary vector pH35G. These vectors were introduced into *Agrobacterium tumefaciens* strain GV3101::pMP90 and then into *rpk2-2* plants using the floral dip method (Clough and Bent, 1998).

Microscopic analyses

Scanning electron microscopic (SEM) analysis was performed as described previously (Kinoshita et al., 2007). In situ hybridization was performed according to the previous report (Hejatko et al., 2006) but using 8 μm sections. The *RPK2* antisense probe was generated from the 1791 bp fragment amplified by PCR using the primers 5′-GCTAGCTG-GGTCGAAGAGA-3′ and 5′-CAAAGCTGCCATCTTCTTCC-3′. The *CLV3* antisense probe was obtained from the 721 bp fragment amplified by PCR using the primers 5′-ATGGATTCGAAGAGTTTTCTG-3′ and 5′-CTTCAGCAACAAACGTAATG-3′. The *WUS* antisense probe was generated as described previously (Mayer et al., 1998).

For GFP analysis, aerial parts of plant materials were embedded in 5% agarose and sliced. Longitudinal sections (50 μm) were mounted in water and the GFP fluorescence was observed by confocal laser scanning microscopy (TCS SP, Leica Microsystems, Heidelberg, Germany). Root samples were directly mounted in water and the GFP signal was detected.

Gene expression analyses

Total RNA for quantitative RT-PCR was isolated from inflorescence meristems with stage 6 and earlier flowers using TRIzol Reagent (Invitrogen). Dissolved RNA samples were subjected to on-column DNA digestion with the RNase-free DNase set (QIAGEN, Hilden, Germany), and cleaned up with the RNeasy spin column (QIAGEN). One μg of total RNA were used for generating the first-strand cDNA using Superscript III (Invitrogen). Quantitative RT-PCR analysis was conducted on a Roche LightCycler using the LightCycler TaqMan Master (Roche Diagnostics, Basel, Switzerland), 1 μl out of 20 μl of RT reaction and the following primer-probe pairs: CLV3-155F (5′-GACTTTCCAACCGCAAGATG-3′), CLV3-155R (5′-TCATGTAGTCCTAAACCCTTCGT-3′) and probe #155 for *CLV3*; WUS-33F (5′-AACCAAGACCATCATCTCTATCATC-3′), WUS-33R (5′-TCAGTACCTGAGCTTGCATGA-3′) and probe #33 for *WUS*; and TUA4-22F (5′-TCTTGAACATGGCATTCAGC-3′), TUA4-22R (5′-CGGTTTCACTGAAGAAGGTGTT-3′) and probe #22 for *TUA4* (*TUBULIN ALPHA-4 CHAIN*) as a control (Universal Probe Library, Roche Diagnostics). Standard curves were constructed using purified PCR fragments of each gene-coding region.

Transient expression in *Nicotiana benthamiana*

Constructs were made using primers and vectors listed in Table S2 in the supplementary material. *A. tumefaciens* strains GV3101 MP90 or MP90RK carrying expression constructs were grown in YEB media with appropriate antibiotics, harvested by centrifugation at 2600 ***g*** for 10 minutes, and resuspended in infiltration buffer [10 mM MES (pH 5.7), 10 mM $MgCl_2$, 150 μM acetosyringone]. The cultures were adjusted to an OD600 of 1.0 and incubated at room temperature, at least, for 3 hours prior to infiltration. Equal volumes of cultures of different constructs were mixed for co-infiltration, and then mixed with agrobacterial cultures (OD600 of 1.0) carrying p19 silencing suppressor in a 1:1 ratio (Voinnet et al., 2003). The resulting cultures were infiltrated into leaves of 3- to 4-week-old *N. benthamiana*. The leaf samples were harvested 3 days after infiltration for subsequent protein extraction.

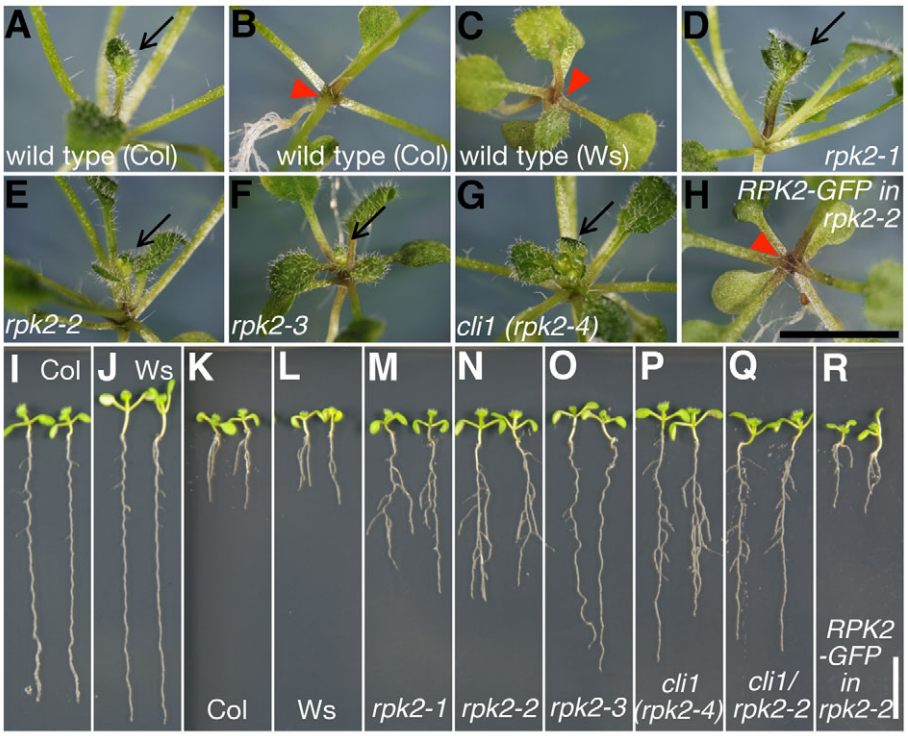

Fig. 1. The *cli1/rpk2* mutants are insensitive to MCLV3 treatment. (**A-H**) Twenty-day-old seedlings of wild-type (Col; A,B), *rpk2-1* (D), *rpk2-2* (E), *cli1* (designated as *rpk2-4*) (G) and *rpk2-2* transformed with the *pRPK2::RPK2:GFP* (H); and 14-day-old seedlings of wild type (Ws) (C) and *rpk2-3* (F). Plants were grown on agar medium with (B-H) or without (A) 5 μM MCLV3. Black arrows indicate the inflorescence meristem regions, and red arrowheads indicate no apical meristem phenotype. (**I-R**) Eight-day-old seedlings of wild type (Col: I, K; Ws: J, L), *rpk2-1* (M), *rpk2-2* (N), *rpk2-3* (O), *cli1* (*rpk2-4*; P), *cli1/rpk2-2* (designated as *rpk2-4/rpk2-2*) (Q) and *rpk2-2* transformed with the *pRPK2::RPK2:GFP* (R). Plants were grown on agar medium with (K-R) or without (I,J) 5 μM MCLV3. Scale bars: 5 mm in A-H; 1 cm in I-R.

Co-immunoprecipitation

Total protein was extracted from 0.5 g of infiltrated *N. benthamiana* leaves with 1 ml of extraction buffer [50 mM Tris-HCl (pH 8.0), 150 mM NaCl, 10% glycerol, 1% Triton X-100, 10 mM NaF, 0.1 mM Na_3VO_4, 1× Proteinase inhibitor cocktail SIGMA P9599 and 1 mM EDTA]. The lysates were centrifuged at 20,000 ***g*** for 20 minutes at 4°C and the supernatants were then centrifuged again at 20,000 ***g*** for 5 minutes at 4°C. The resulted supernatants were incubated with respective antibodies for 1 hour in a rotary shaker at 4°C. Protein G sepharose (Roche 17-0618-01) was then added to the samples and the samples were incubated in a rotary shaker at 4°C overnight. The sepharose beads were collected and washed four times with 1 ml of the extraction buffer. Immunoprecipitated proteins were eluted by boiling in SDS sample buffer at 95°C and analysed on western blot using corresponding antibodies. We used the following antibodies: anti-HA 3F10 (Roche, 1867423), anti-Myc 9E10 (Sigma, M4439) and anti-FLAG M2 (Sigma, F3165).

RESULTS

The CLV3 peptide acts through the endogenous CLV3 pathway involved in SAM regulation

Previously, we have shown that the synthetic CLV3 dodecapeptide (MCLV3) is able to restrict the size of the SAM, however, the molecular basis for the MCLV3-induced SAM defect was yet unknown (Kondo et al., 2006). Here, our bioassay using the synthetic MCLV3 confirmed that the exogenously applied MCLV3 mimics endogenous *CLV3* overexpression to restrict the size of the SAM after *WUS* depression through the functions of CLV1 and CLV2 (see Fig. S1 in the supplementary material). We have also observed a similar trend in the bolting phenotype, when growing plants on a solid medium supplied with MCLV3, enabling us to perform simple chemical genetics screenings on MCLV3 solid media (see Table S1 in the supplementary material).

In order to identify novel molecular components operating in the CLV3 signalling pathway, we have performed mutational screens for insensitivity to MCLV3 on ~10,000 M_2 plants derived from EMS-mutagenised *Arabidopsis* seed pools. A total of 14 mutants, designated *clv3 peptide insensitive* (*cli*) mutants, were isolated for maintaining the SAM when grown on agar media containing 5 μM MCLV3. Among them, *cli1* mutant showed the strongest resistance to the MCLV3. When grown on agar plate containing 5 μM MCLV3, *cli1* plants were able to maintain the SAM activity and to induce bolting, whereas the wild type failed to bolt (Fig. 1A,B,G). In addition, similar to *clv2* and *crn/sol2*, *cli1* suppresses not only the SAM defects, but also the short-root phenotypes caused by the MCLV3 application (Fig. 1I,K,P). These data indicate that *CLI1* is required for MCLV3-mediated signalling to restrict the meristem size both in the shoot and the root, similar to *CLV2* and *CRN/SOL2*.

The F_1 progeny of *cli1* crossed to Col was sensitive to the MCLV3. In the following F_2 population, about one-quarter (6/30) of the offspring showed MCLV3 resistance, which indicates that the *cli1* phenotype was caused by a single recessive mutation.

CLI1 encodes a leucine-rich repeat receptor like kinase

The *cli1* mutation was mapped to a single locus on chromosome 3. Fine mapping located the gene between 74683 bp of BAC F28J7 and 55403 bp of BAC F14P3 (see Fig. S2A in the supplementary material). The DNA sequencing of this region identified a nucleotide exchange from G to A at 2656 bp from the start codon of *At3g02130*, which causes substitution of Gly886 with an arginine at the putative ATP-binding site of the predicted protein (see Fig. S2B in the supplementary material). *At3g02130* encodes an LRR-RLK and has been reported as *RECEPTOR-LIKE PROTEIN KINASE 2* (*RPK2*) (Mizuno et al., 2007) or *TOADSTOOL 2* (*TOAD2*) (Nodine et al., 2007). Previous reports have demonstrated that RPK2 is a key regulator of another development (Mizuno et al., 2007) and functions redundantly with RPK1 to coordinate central domain protoderm patterning during the late globular stage (Nodine et al., 2007). However, it is not known whether the *RPK2* gene is required for meristem development, similar to the CLV pathway. To determine whether *RPK2* is the causal gene for the *cli1* phenotype,

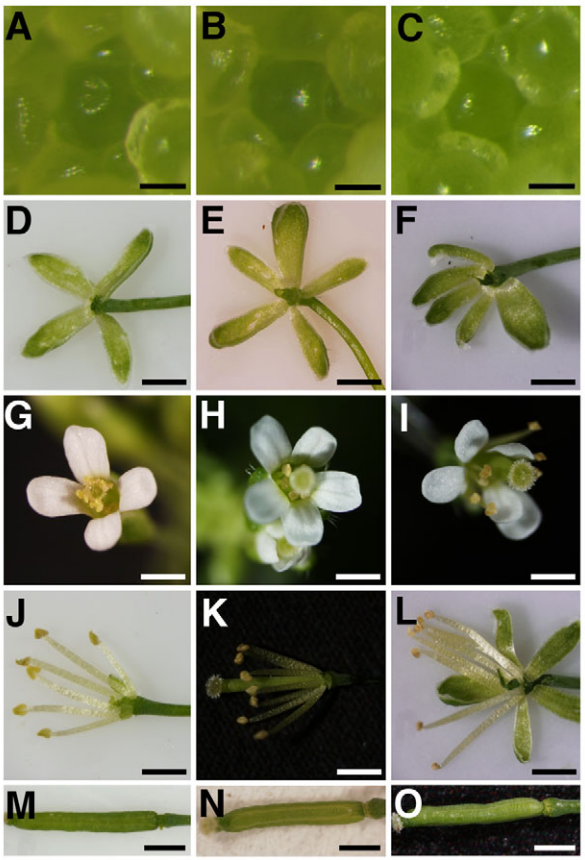

Fig. 2. Phenotypes of *rpk2* mutants in the absence of exogenous MCLV3 peptides. (**A-C**) Inflorescence meristems of wild type (Col; A), *rpk2-2* (B) and *rpk2-4* (C) grown under continuous light for 6 weeks. (**D-O**) Floral organs of wild type (D,G,J,M), *rpk2-2* (E,H,K,N) and *rpk2-4* (F,I,L,O). Increased numbers of sepals (D-F), petals (G-I), stamens (J-L) and carpels (M-O) are observed in *rpk2-2* and *rpk2-4*. Scale bars: 50 μm in A-C; 1 mm in D-O.

T-DNA insertion *rpk2* mutant alleles, *rpk2-1*, *rpk2-2* (Col background) and *rpk2-3* [Wassilewskija (Ws) background], were tested for sensitivity to the MCLV3. When seedlings of these lines were grown with MCLV3, all of these alleles were resistant to the MCLV3 in both the shoot (Fig. 1A-F; see Fig. S3D,H in the supplementary material) and the root (Fig. 1I-O; see Fig. S4I in the supplementary material). Furthermore, the *cli1/rpk2-2* heterozygotes also showed resistance against peptide treatment (Fig. 1Q; see Fig. S4I in the supplementary material), while the transgenic *rpk2-2* plants, in which the *pRPK2::RPK2-GFP* construct was introduced, were sensitive to MCLV3 (Fig. 1H,R; see Fig. S4I in the supplementary material). We therefore concluded that *cli1* is allelic to *rpk2*, and hereafter refer to *cli1* as *rpk2-4*. Furthermore, a mutation in the *RPK1* gene, which shares high sequence similarity with *RPK2*, did not suppress the effect of MCLV3 (see Fig. S4I in the supplementary material). This suggests that the *RPK2* is the specific gene that functions in meristems, and participates in a CLV3 signalling pathway.

Phenotypes of *rpk2* mutants in the absence of exogenous MCLV3 peptides

In order to decipher the functions of *RPK2* in meristem and flowers in more detail, we observed the phenotypes of *rpk2* plants grown under MCLV3-free condition. Although the size of the inflorescence meristem of *rpk2* was not strongly affected (Fig. 2A-C), the size of the *rpk2* vegetative SAM was slightly enlarged (see Fig. S9A-C in the supplementary material). In addition, the numbers of floral organ in all four whorls of *rpk2-2* and *rpk2-4* was occasionally increased, compared with the typical 4-4-6-2 pattern of the wild type (Fig. 2D-O). To quantify the effect of *rpk2* on the floral meristem, we counted the number of carpels, which has been established as a good indicator for the *clv* phenotype (Ni and Clark, 2006). In contrast to the wild-type flowers producing invariantly two carpels per flower, *rpk2-1*, *rpk2-2* and *rpk2-4* developed an increased number of carpels (Table 1). Comparing with *clv1*, *clv2* or *crn/sol2*, the *rpk2* mutation is weak and impenetrant but statistically distinct from the wild type. The phenotype was often observed in the flowers generated at the basal part of the inflorescence in *rpk2-2*, and *rpk2-4* produced the abnormal flowers constantly (see Fig. S4A-D in the supplementary material). The severe phenotype was also observed just before the termination of the inflorescence meristem (see Fig. S4E-G in the supplementary material), and the *rpk2-4* flowers often developed carpels interior to the whorl 4 gynoecium (see Fig. S4H in the supplementary material).

Table 1. Number of carpels in various mutants

Genotype	Carpels per flower	SE	*n*	Valveless siliques (%)*
Col	2.0	0.0	100	N/D
rpk2-1	2.2	0.0	150	N/D
rpk2-2	2.2	0.1	90	N/D
rpk2-4	2.6	0.1	110	0.9
rpk2-2/rpk2-4	2.5	0.1	90	1.1
RPK2/rpk2-4	2.0	0.0	100	N/D
clv1-101	3.2	0.1	120	N/D
clv2-101	2.5	0.1	50	N/D
clv3-8	3.9	0.1	120	2.5
clv1-101 rpk2-2	3.5	0.1	80	2.5
clv2-101 rpk2-2	3.2	0.1	100	12.0
clv1-101 clv2-101	3.1	0.1	190	5.8
clv1-101 clv2-101 rpk2-2	3.1	0.1	190	32.1

*Percent of flowers with gynoecia in which the basal 25% completely lacked valves.

In the root, all the *rpk2* alleles were resistant to MCLV3. As in the carpel number phenotypes, *rpk2-4* showed the strongest resistance (see Fig. S4I in the supplementary material). In contrast to the *rpk2* phenotypes in the floral organ, *rpk2* mutants do not exhibit any obvious morphological alterations in the root when grown without the peptide (data not shown). This observation again led us to the idea that *rpk2* shares similarities with *clv2* and *crn/sol2* that also do not show any morphological root phenotype per se (Kayes and Clark, 1998; Miwa et al., 2008; Müller et al., 2008). Taken together, our data indicate that RPK2 contributes to CLV3 signalling in the SAM and may compose a CLV-like pathway together with CLV2 and CRN/SOL2 acting in the RAM.

Expression of *RPK2*

Analyses of *pRPK2::GUS* transgenic plants have shown *RPK2* expression in the root tips and the shoot meristems (Mizuno et al., 2007). In order to dissect further the spatial pattern of the *RPK2* expression, we performed in situ mRNA hybridization experiments. Expression of *RPK2* was observed in the inflorescence meristem, floral meristem, floral organ primordium, the vascular bundles and the RAM region (Fig. 3A-E). The serial sections of the inflorescence meristem detected the *RPK2* transcripts uniformly through the inflorescence meristem (Fig. 3B). In the RAM, *RPK2* signal was detected through the RAM,

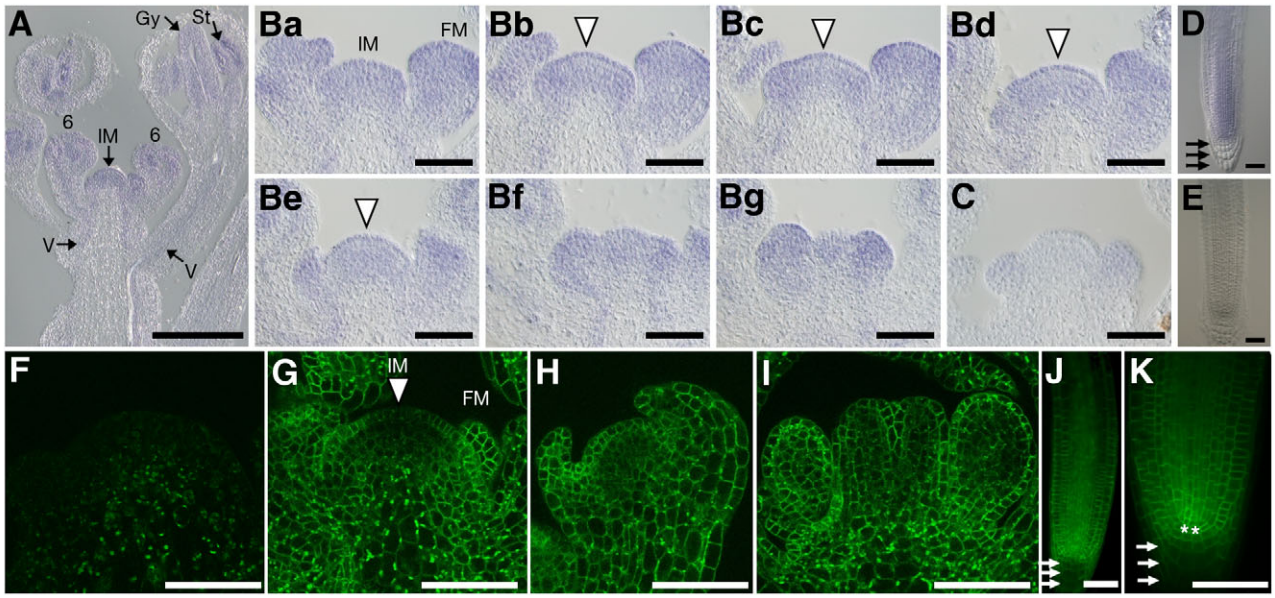

Fig. 3. *RPK2* expression in the shoot and root apical meristems. (**A-E**) RNA in situ hybridization performed using the *RPK2* antisense probe. SAM sections of wild type (Col; A, serial sections: B1-B7) and *rpk2-2* (C), and the whole-mount root meristems of wild type (Col; D) and *rpk2-2* (E). (**F-K**) GFP signals of inflorescence meristem (G), stage 3 flower (H), stage 7 flower (I) and root meristems (J,K) in *pRPK2::RPK2:GFP* transgenic plant. The autofluorescence of chloroplasts is also detected in the Col wild type (F) with the same microscopic condition, and the signal at the plasma membrane is specifically detected in the transgenic plant (G-K). IM, inflorescence meristem; FM, floral meristem; asterisk, quiescent centre; arrows, columella cells. White arrowheads indicate the central zone. Scale bars; 200 μm (A), 50 μm (B-K).

including initial cells and the QC but not the columella cells (Fig. 3D). We also assessed the localization of RPK2 protein using the stable transgenic *Arabidopsis* expressing functional RPK2-GFP fusion protein under the control of the own promoter. In contrast to the uniform distribution of the *RPK2* transcripts, confocal microscopic analysis showed that the RPK2-GFP fusion protein is preferentially detected in the PZ and rather weakly in the CZ (Fig. 3F-I). In the RAM, however, the RPK2-GFP is detected similarly with the RPK2 transcript (Fig. 3J,K). Together with the *rpk2* phenotypic data, these results suggest that *RPK2* may function as a signalling molecule in both SAM and RAM maintenance mediated by endogenous CLV3 or a CLV3-related CLE peptide.

Overexpression of *RPK2* phenocopies *CLV3* overexpressing plants and *wus* mutants

We then investigated the roles of RPK2 activity in SAM and RAM maintenance using *Arabidopsis* stable transgenic lines constitutively overexpressing the *RPK2* gene under the control of the cauliflower mosaic virus 35S promoter (*RPK2* OX). The *RPK2* OX plants occasionally showed developmental arrest of SAM growth, which resembles the MCLV3-treated plants, *CLV3* OX plants and *wus* mutants (Fig. 4A,B; see Fig. S5A in the supplementary material). The RAM of the *RPK2* OX transgenic lines was diminished compared with the wild type (Fig. 4I,J) and resulted in a short-root phenotype (Fig. 4K,L). In addition, the *RPK2* OX transgenic plants occasionally produced flowers with reduced floral organ numbers (Fig. 4C-H), and the abnormal flower phenotypes were mainly observed in the central region, carpels and stamens, as typically observed in *CLV3* OX lines and *wus* mutants (Brand et al., 2000; Laux et al., 1996). It should be noted that degrees of all the abnormalities of the *RPK2* OX lines are strongly coincident with the *RPK2* expression levels in the individual lines (see Fig. S5B in the supplementary material). These phenotypes of the *RPK2* OX plants are consistent with the *rpk2* mutant phenotype. The data prompted us to conclude that *RPK2* is a component of the *CLV3-WUS* feedback loop.

Expressions of shoot meristem marker genes in *rpk2*

Given its identity as an LRR-RLK, we hypothesised that RPK2 functions closely together with other known receptors to transmit the CLV3 signal. To examine this hypothesis, we compared the phenotype of *rpk2*, *clv1* and *clv2*. *clv1-101* and *clv2-101* are the presumed null alleles of *CLV1* and *CLV2*, respectively, both in Col background, and these mutants show a weak *clv* phenotype (see Fig. S3A-C; Fig. S6 in the supplementary material). Histological analysis revealed that the expression regions of both *CLV3* and *WUS* are enlarged in *clv1-101* and *clv2-101* (Fig. 5A-C,E-G), which is consistent with the previous reports for La-*er* alleles. By contrast, these expression regions are almost normal or slightly expanded in *rpk2-2* (Fig. 5D,H). Quantitative RT-PCR confirmed that the expression level of *CLV3* in *rpk2-2* is slightly upregulated compared with wild type, but less strongly upregulated than in *clv1-101* or *clv2-101* (Fig. 5I). These results correlate with the severity of the mutant phenotype. Interestingly, although its expression regions are enlarged, *WUS* expression levels in *clv1-101* and *clv2-101* are only slightly affected (Fig. 5J).

Genetic interaction between *CLV1*, *CLV2*, *WUS* and *RPK2*

In order to examine the relationship among CLV1, CLV2 and RPK2, we constructed double and triple mutants of these three genes. To avoid any interfering effects as known for *clv1* alleles (Diévart et al., 2003), null alleles in Col background were chosen for the crossing. First, we observed the inflorescence meristem of bolting plants. As reported for La-*er* alleles before, *clv1-101* and *clv2-101* produced

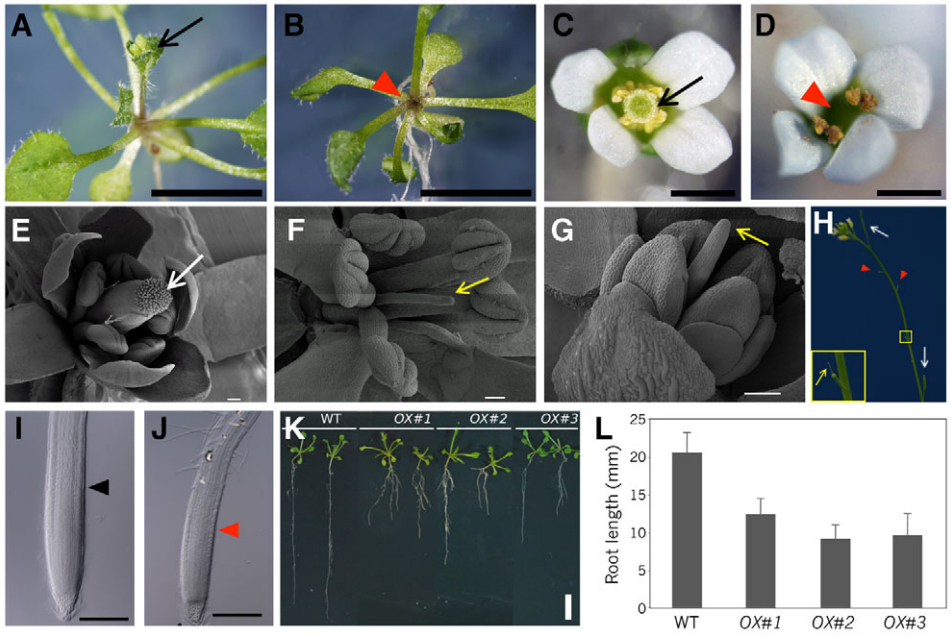

Fig. 4. Overexpression of the *RPK2* gene mimics *CLV3* overexpression. (**A**,**B**) Twenty-day-old seedlings of wild type (Col; A) and *RPK2 OX* plant (B). Black arrow indicates inflorescence stem, whereas the red arrowhead indicates 'no apical meristem' phenotype. (**C-H**) Mature flowers of wild type (Col; C,E) and *RPK2 OX* (D,F,G,H). Black and white arrows indicate intact pistils; red arrowheads indicate no-pistil phenotype; yellow arrowheads indicate pin-shaped pistils. A magnified view is shown in the inset (H). (**I**,**J**) Root meristems of wild type (Col; I) and *RPK2 OX* (J). Arrowheads show the RAM areas. (**K**) Fourteen-day-old seedlings of wild type and three independent lines of *RPK2 OX*. Main roots of *RPK2 OX* plants are shorter than wild type. (**L**) Main root length of 7-day-old seedling. Scale bars: 1 cm in A,B; 1 mm in C,D; 100 μm in E-G; 200 μm in I,J; 1 mm in K.

larger SAM than wild type (Fig. 6A-C), but rarely fasciated under long-day conditions. However, *clv1-101 clv2-101*, *clv1-101 rpk2-2* and *clv2-101 rpk2-2* double mutants exhibited larger SAM than any single mutants (Fig. 6B,C,E-J). Especially, four out of nine and three out of five SAM were fasciated in *clv1-101 clv2-101* and *clv1-101 rpk2-2*, respectively (Fig. 6G,J). Furthermore, *clv1-101 clv2-101 rpk2-2* triple mutant showed not only the fasciated SAM (3 out of 12; Fig. 6K), but also the massively overproliferated SAM, as seen in *clv3* single mutants (eight out of 12; Fig. 6D,L). A similar trend was observed for 7-day-old vegetative SAMs of each mutant (see Fig. S7A-C in the supplementary material), and the SAM of *clv1-101 clv2-101 rpk2-2* triple mutants is similar in size to that of *clv3-8*. We next examined the effect of the *rpk2* mutation on the *clv1* or *clv2* floral meristems. Compared with each single mutant, carpel numbers were increased from 3.4 to 4.0 in *clv1-101 rpk2-2*, and from 2.3 to 3.0 in *clv2-101 rpk2-2* (Table 1). In addition, as reported, a fifth whorl of organs was observed in *clv1-101*, *clv2-101*, *clv1-101 rpk2-2* and *clv2-101 rpk2-2*. However, only the double mutant of *clv1-101 rpk2-2* and *clv2-101 rpk2-2* exhibited externally emerged, highly proliferated fifth whorls (Fig. 6M-P), indicating that *rpk2* is additive with *clv1* or *clv2* in the floral meristem phenotype. Unexpectedly, however, *clv1-101 clv2-101* double mutant and *clv1-101 clv2-101 rpk2-2* triple mutant had fewer carpels than the *clv1-101* single mutant (Table 1). This may be due to the valveless phenotype (Fig. 6Q-S), which is often seen in *clv2* and *clv1* severe alleles (Diévart et al., 2003; Kayes and Clark, 1998). Alternatively, it is also possible that these receptors redundantly function in fruit development other than the floral meristem regulation. These data suggest that RPK2 functions independently of CLV1 or CLV2 in both inflorescence and floral meristems.

In order to position *RPK2* genetically in the *CLV3-WUS* signalling, we tested the effect of *WUS* in the *rpk2-2* background. As observed in the *wus-101* single mutant, the *wus-101 rpk2-2* double mutant exhibited a terminated SAM (see Fig. S8A-C in the

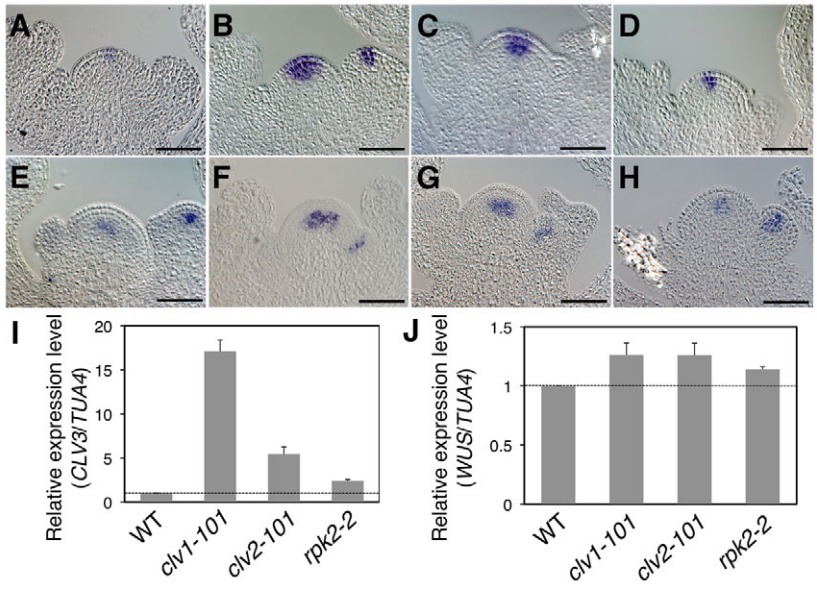

Fig. 5. *WUS* and *CLV3* expression in *rpk2* mutants. (**A-H**) RNA in situ hybridization was performed with the meristem sections of wild-type (A,E), *clv1-101* (B,F), *clv2-101* (C,G) and *rpk2-2* (D,H) using the *CLV3* antisense probe (A-D) and the *WUS* antisense prove (E-H). (**I**,**J**) Relative expression levels of *CLV3* (I) and *WUS* (J) against *TUA4*. Scale bars: 50 μm (A-H).

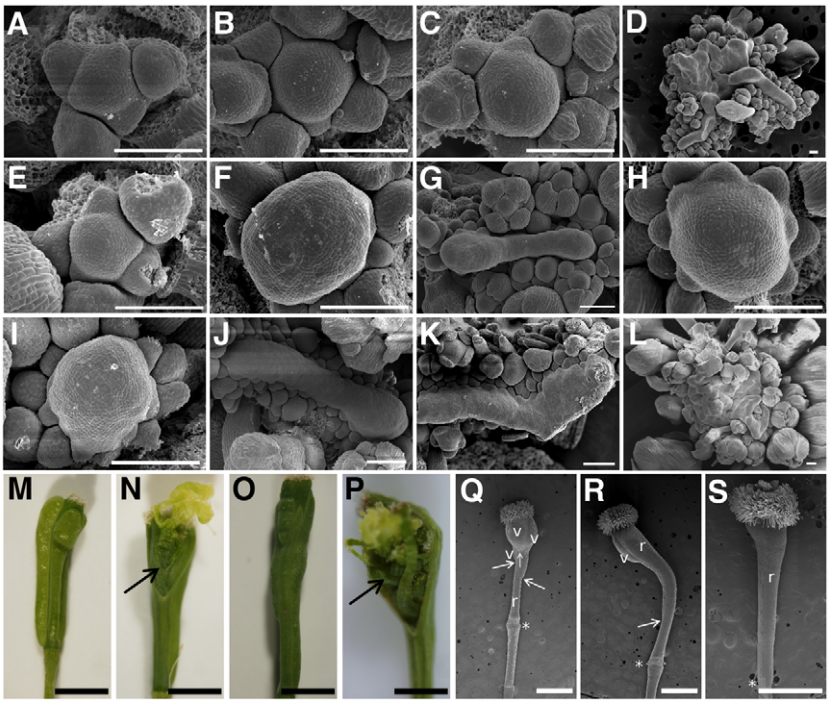

Fig. 6. Genetic interactions of *RPK2*. (**A-L**) Scanning electron micrographs of wild type (Col; A), *clv1-101* (B), *clv2-101* (C), *clv3-8* (D), *rpk2-2* (E), *clv1-101 rpk2-2* (F,G), *clv2-101 rpk2-2* (H), *clv1-101 clv2-101* (I,J) and *clv1-101 clv2-101 rpk2-2* (K,L). (**M-S**) Mature siliques of *clv1-101 rpk2-2* (M,N), *clv2-101 rpk2-2* (O,P) and *clv1-101 clv2-101 rpk2-2* (Q-S). v, valve; r, replum; arrow, valve end; asterisk, attachment site for the sepals, petals and stamens. Scale bars: 100 μm in A-L; 1 mm in M-S.

supplementary material). Furthermore, *35S::WUS* in *rpk2-2* transgenic plants produced the larger SAMs, resulting in stem fasciation (see Fig. S8D-G in the supplementary material). Thus, these genetic data strongly suggest that *WUS* is epistatic to *RPK2*.

Biochemical interaction of RPK2 with CLV1 and CLV2

Our genetic data suggested that RPK2 functions in parallel with CLV1 and CLV2 to restrict *WUS* expression in the SAM. To further provide an evidence for our genetic data on RPK2 function, we next investigated biochemically whether RPK2 associates with CLV1 or CLV2-CRN/SOL2 complexes using the *Agrobacterium tumeafaciens*-mediated transient expression system in *Nicotiana benthamiana* leaf epidermis. The *N. benthamiana* system has been established to demonstrate that CLV1 homo-oligomer and CLV2-CRN/SOL2 hetero-oligomer co-exist at the plasma membrane by FRET analysis, consistent with genetically proposed two independent CLV3 signalling pathways. These two complexes are capable of interacting weakly with each other, suggesting a potential crosstalk (Bleckmann et al., 2010; Zhu et al., 2009).

First, we co-expressed CLV1 C-terminally fused to triple HAs-single StrepII (CLV1-3HS), CLV2 with triple FLAGs (CLV2-3FLAG) and CRN/SOL2 with 10 times Myc (SOL2-10Myc), under the control of the 35S promoter. Co-immunoprecipitation using anti-Myc antibody detected CLV2-FLAG, but failed to detect CLV1-3HS, showing that CLV1 complex and CLV2-CRN/SOL2 complex co-exists in *N. benthamiana* (Fig. 7A). This is consistent with previous genetic data using *A. thaliana* and microscopic data in *N. benthamiana*, and validates our biochemical interaction assay in *N. benthamiana*.

Then, we co-expressed RPK2 fused to 10 times Myc with CLV1-3HS and RPK2 fused to triple HA (3HA) with CLV2-3FLAG. In co-immunoprecipitation experiments using anti-Myc, we did not detect interaction of RPK2-10Myc with CLV1-3HS (Fig. 7B). Interaction between RPK2-3HA and CLV2-3FLAG was also undetectable in co-immunoprecipitation using anti-HA (Fig. 7C). The biochemical data suggests that RPK2 is not included in the previously shown CLV1 complex or CRN/SOL2-CLV2 complex, at least, under our experimental conditions. However, when RPK2-10Myc was co-expressed with RPK2-3HA, RPK2-10Myc was co-immunoprecipitated with RPK2-3HA (Fig. 7D). Taken together, our biochemical study on RPK2 interactions in *N. benthamiana* demonstrated that RPK2 can form homo-oligomers, independently of CLV1 or CRN/SOL2-CLV2 complexes.

DISCUSSION

Via mutational screening using synthetic MCLV3 peptide, we have identified RPK2 as a novel regulator of plant meristem maintenance. Although previous studies have shown that RPK2 operates in anther and embryo development, our findings have uncovered additional roles for RPK/TOAD2 in SAM and RAM maintenance. Furthermore, our genetic studies indicate that RPK2 transmits the CLV3 signal in the SAM, independently of the two previously known CLV3 signalling pathways: the CLV1 and the CLV2-CRN/SOL2 pathways. The existence of these three major CLV3 receptor complexes was further supported by our transient in planta interaction assay using *N. benthamiana*.

RPK2 function in the CLV3 signalling

The *rpk2* mutant shows defects both in fertility and floral organ number. Previous studies, however, have not mentioned the latter phenotype (Mizuno et al., 2007; Nodine et al., 2007). The null alleles of *rpk2* by T-DNA insertions exhibit a weak and impenetrating phenotype and, furthermore, the male sterile nature of the *rpk2* plants results in relatively small siliques, which makes it difficult to observe the typical club-shaped siliques. However, in this screening, we have isolated a new strong *rpk2* allele, *rpk2-4*, which exhibits a consistently severe phenotype in floral organ number. The abnormal club-shaped siliques of this mutant then enabled us to notice the more subtle phenotypes of the null alleles. Previous reports suggest that specific *clv1* alleles act semi-dominantly and interfere with other RLK(s) function, resulting in

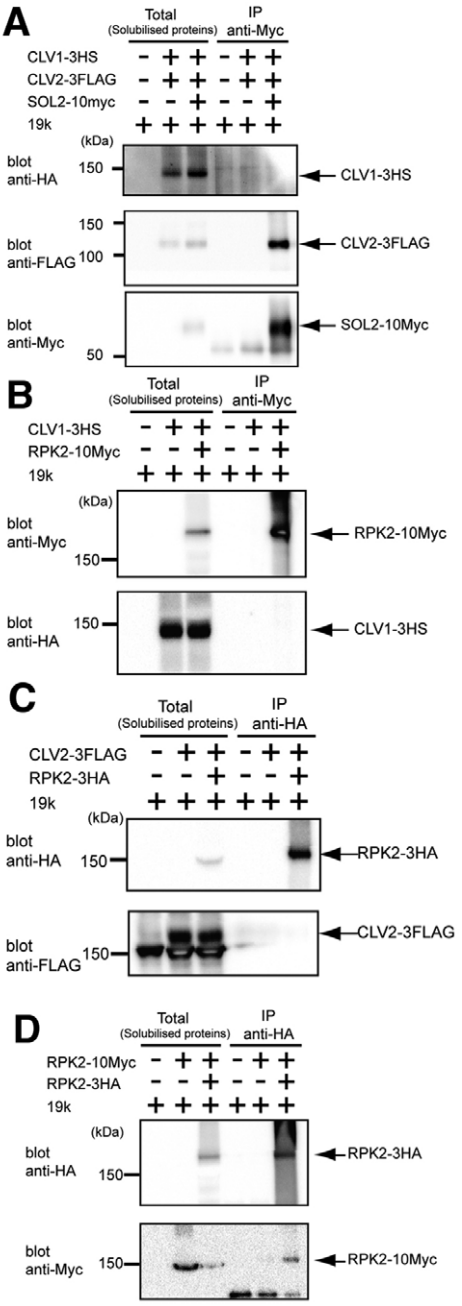

Fig. 7. Biochemical interactions of RPK2. (**A**) Interaction assay using CLV1-3HS, CLV2-3FLAG and CRN/SOL2-10Myc in *N. benthamiana*. These constructs co-expressed in *N. benthamiana*, and total protein extracts were subjected to immunoprecipitation using anti-Myc antibody. The resultant immuno-complexes were analysed on western blot with anti-Myc, anti-HA or anti-FLAG antibody. CLV2-3FLAG, but not CLV1-3HS, was specifically co-immunoprecipitated with CRN/SOL2-Myc, validating our biochemical interaction assay in *N. benthamiana*. This experiment was repeated at least twice with similar results. (**B-D**) Interaction assay of RPK2. RPK2-10Myc was co-expressed with CLV1-3HS (B), RPK2-3HA was co-expressed with CLV2-3FLAG (C) and RPK2-3HA (D) in *N. benthamiana*. This experiment was repeated at least three times with similar results.

stronger phenotypes than the null allele of *clv1* (Diévart et al., 2003). Considering that *rpk2-4* has a point mutation at the putative ATP binding site of RPK2 protein, it could interrupt other functional protein kinase such as CLV1 or CRN/SOL2, and could interfere with the downstream signal in a similar fashion to the strong *clv1* alleles.

Our genetic analysis indicated that RPK2 comprises the third pathway to transmit the CLV3 signal along with the CLV1 and CLV2-CRN/SOL2 complexes. We did not include *CRN/SOL2* in our genetic study; however, it has been established that *CRN/SOL2* acts together with *CLV2*, at least, in the regulation of the inflorescence and the floral meristems (Müller et al., 2008). Based on these established data, we used the *clv2* mutant as a genetic marker of the *CLV2-CRN/SOL2* pathway. Additionally, we analysed the phenotype of the double mutant of the *clv1* null and *clv2* null alleles, and we confirmed, for the first time, the additivity of the double mutant phenotype as suggested previously (Müller et al., 2008). Notably, our quantitative data revealed that any double mutant combinations among *clv1*, *clv2* and *rpk2* are additive; however, the triple mutant appears to be synergistic (see Fig. S7 in the supplementary material). Considering that the triple mutant is almost equivalent to *clv3-8*, the remaining receptor(s) in the single and double mutants might functions to over-activate *CLV3* expression via increased *WUS* expression (Fig. 5), resulting in masking the effect of the loss of the receptor(s). The *rpk2* mutant exhibits the weaker *clv*-like phenotype compared with the *clv1* or *clv2* mutants; however, RPK2 should play a minor but indispensable role in the SAM homeostasis along with CLV1, CLV2 and CRN/SOL2.

Recent study suggested that CLV1-related LRR-RLKs, BAM1 (for BARELY ANY MERISTEM) and BAM2 exert a function to sequester the CLE in the PZ of the SAM (DeYoung and Clark, 2008). The *bam1 bam2* double mutant shows male sterility and enhances the *clv1* phenotype (DeYoung and Clark, 2008; Hord et al., 2006), both of which are also observed in *rpk2*. However, *rpk2* interacts additively with *clv2* for the floral meristem phenotypes, while *bam1 bam2* double mutant does not. CLV1 shares high sequence similarities with BAM1 and BAM2, whereas RPK2 belongs to a distinct subfamily of LRR-RLKs in the *Arabidopsis* genome (DeYoung and Clark, 2008; Shiu and Bleecker, 2001). With these points, we conclude that RPK2 function in the SAM is unlikely to overlap with BAM1 and BAM2 activities but is similar to CLV1, CLV2 and CRN/SOL2 functions.

We have revealed that *RPK2* is required for exogenously applied MCLV3 mediated-reduction of the SAM size and the root length. However, we do not know exactly whether RPK2 participates in CLV3 recognition. Owing to the technical difficulties in synthesizing arabinosylated CLV3, the most likely mature form of CLV3 in planta, it is still unclear whether RPK2 directly binds to the endogenous CLV3, as shown for CLV1 (Ogawa et al., 2008; Ohyama et al., 2009). It is possible that RPK2 perceives, instead of CLV3, other CLE(s) expressed in the SAM to regulate the meristem (see Fig. S7 in the supplementary material). In fact, there are several *CLE* genes other than *CLV3* expressed in the shoot apex (Sharma et al., 2003; Yadav et al., 2009), one of which, *CLE40*, displays a similar expression pattern to *RPK2* (Hobe et al., 2003). In addition, *rpk2* shows resistance not only to the MCLV3, but also to the other CLE peptides (at least 14 of CLE peptides tested so far; A.K., unpublished data). However, it might be difficult to define a specific ligand for RPK2, as biochemical study revealed that multiple CLE peptides can bind to the CLV1 extracellular domain with different affinity, suggesting that CLV1 might recognizes multiple CLE expressed in the SAM (Ohyama et al., 2009). In the same context, RPK2 may recognize multiple CLEs, including CLV3 in the SAM.

Consistent with our genetic data, our biochemical data revealed that RPK2 does not associate with CLV1 or CLV2, instead, forms a homo-dimer (oligomer) in *N. benthamiana*, indicating that RPK2 is likely to comprise the third receptor complex in the SAM of *A. thaliana*, independently of CLV1 and CLV2-CRN/SOL2 complexes. RPK2 homo-oligomerization occurs independently of the MCLV3 application; however, we cannot rule out the possibility that RPK2 homo-oligomerization might be triggered upon recognition of CLV3-like CLE peptide derived from *N. benthamiana* leaf tissue. Recent studies using fluorescent-tagged CLV receptors revealed that CLV1 homomer and CLV2-CRN/SOL2 heteromer co-exist, independently of the CLV3 peptide, at the plasma membrane, and that these two complexes are able to associate together, presumably through a weak interaction between CLV1 and CRN/SOL2 (Bleckmann et al., 2010). Our co-immunoprecipitation using anti-myc did not detect a clear strong interaction between CLV1-3HS and CLV2-3FLAG-CRN/SOL2-10Myc complexes, probably owing to the sensitivity limit of co-immunoprecipitation experiment in our buffer condition, compared with fluorescence-based cell biology techniques. It is also possible that the association between CLV1 and CLV2-CRN/SOL2 complexes might be very transient and dynamic. This type of interaction might be very difficult to detect with co-immunoprecipitation.

Taken together, we propose that, independently of CLV3 ligand stimuli, there are three stable CLV3 receptor complexes at the surface of the SAM cells of *A. thaliana*: CLV1 homomer, CLV2-CRN/SOL2 heteromer and RPK2 homomers. These three receptor complexes should perceive the CLV3 signal individually to restrict the *WUS* expression. The CLV1 and CLV2-CRN/SOL2 complexes are also likely to associate with each other and RPK2 homo-oligomer might participate in such a formation of the larger complex. The *rpk2-4* alleles, which carries a point mutation at the ATP-binding site of RPK2, might reflect such a crosstalk of RPK2 complex with the CLV1, CLV2-CRN/SOL2 complexes.

One interesting observation is that overexpression of *RPK2* causes the *CLV3*-overexpression phenotype, which is distinct from the situation for CRN/SOL2. This observation possibly suggests that elevated levels of RPK2 protein accumulation might trigger dose-dependent auto-activation of the RPK2 pathway and/or the other pathways. Notably, our microscopic analysis of fluorescent-tagged RPK2 revealed that accumulation of RPK2 protein is relatively low in the CZ (Fig. 3G), whereas *RPK2* transcript distributes almost uniformly in the SAM (Fig. 3B). These data led us to speculate that the lower RPK2-GFP signal in the CZ might reflect highly active internalization and subsequent degradation of RPK2 protein in the CZ, presumably triggered by CLE ligands recognition, as demonstrated for BRI1, BAK1, BOR1 and FLS2 (Chinchilla et al., 2007; Geldner et al., 2007; Robatzek et al., 2006; Takano et al., 2005). Alternative explanation might be that the amount of RPK2 protein is limited in the SAM in ratio to CLE ligands. However, our MCLV3 and the previous CLV3-overexpressing experiments resulted in the termination of the SAM, suggesting that the amount of RPK2 protein is not rate-limiting. Thus, the molecular basis of the *RPK2* overexpression phenotype is still under discussion at this point. A future challenge will be a detailed analysis of the molecular function of RPK2 to gain insights into this interesting phenotype.

Here, we have shown our genetic, biochemical and histological analyses of RPK2 function. However, all the interaction data concerning the CLV receptors, including our data, have been obtained using transient and ectopic overexpression system. These data lack the information on the distribution of these receptor proteins and CLE ligands in the SAM, except for RPK2 shown in this study. Furthermore, downstream direct targets of these receptor complexes are yet unknown. Future detailed analysis of these aspects should enable us to understand precisely the complex signalling machinery comprising these multiple receptors and CLEs in the regulation of the SAM homeostasis.

Additional aspects of RPK2 function

Phenotypic analyses suggest that the RPK2 function is not be restricted in the SAM. Interestingly, the *rpk2* mutants do not exhibit MCLV3-induced short root phenotype. This is also observed in the *clv2* and *crn/sol2* mutants (Fiers et al., 2005; Miwa et al., 2008; Müller et al., 2008). Although none of these single mutants show any morphological phenotypes in the root, the application of CLE peptides apparently affects root architecture in CLV2- and CRN/SOL2-dependent manner. Further detailed genetic analyses would shed some light on CLE signalling in the proximal RAM. Furthermore, besides the MCLV3 resistance, *rpk2* shows multiple phenotypes, including male sterility, smaller rosette leaves, increased branching and spindly shoots (Mizuno et al., 2007; Nodine et al., 2007). Therefore, it would also be interesting to dissect involvement of CLEs in these phenotypes.

Many of the identified and proposed receptors for CLE ligands, so far, fall in the LRR-RLK subclass XI (Clark et al., 1993; DeYoung et al., 2006; Hirakawa et al., 2008; Shiu and Bleecker, 2001), whereas RPK2, CRN/SOL2 and CLV2 do not belong to this class. Interestingly, so far, none of these three receptors has been shown to bind directly to CLE peptides. Therefore, the alternative hypothesis is that RPK2, as well as CLV2 and CRN/SOL2, might contribute to the CLV3-dependent *WUS* suppression signalling by a non-CLE mediated manner. Recent study revealed involvement of cytokinin signalling in addition to CLE40-mediated regulation of the RAM homeostasis (Dello Ioio et al., 2008; Ruzicka et al., 2009; Stahl and Simon, 2009). Cytokinin signalling is known to function in the regulation of the SAM homeostasis (Gordon et al., 2009; Kurakawa et al., 2007; Leibfried et al., 2005). It is possible that RPK2 and, perhaps CLV2 and CRN/SOL2, might transmit non-CLE signal(s), such as cytokinin, to the *CLV3-WUS* signal flow. In this context, the RPK2-containing receptor complex might be a convergent point of different hormone signals, not only CLE but also others, in the regulation of the *WUS* expression levels to achieve an organized and orchestrated development of the SAM. A future challenge would be to identify a direct ligand for RPK2, which should provide further insights in understanding precise signalling machinery in the regulation of the SAM homeostasis.

Acknowledgements

We thank Prof. David Baulcombe for Agrobacterium strain carrying the p19 silencing suppressor; Prof. Jane Parker for Agrobacterium strains GV3101 pMP90RK, pXCSG-3HS and pXCSG-3FLAG; Prof. Tsuyoshi Nakagawa for pGWB binary vectors; and Prof. Taku Demura for pH35G vector. We also thank Prof. Masayoshi Kawaguchi, Dr Masashi Yamada and Mr Hikota Miyazawa for valuable discussion. We appreciate TAIR and GABI-kat for their valuable resources. A.K. was supported by Research Fellow of the Japan Society for the Promotion of Science. This work was supported by: Grant-in Aid for Creative Scientific Research; Grant-in-Aid for Young Scientists S (19677001) from Japan Society of the Promotion of Science; Grant-in-Aid for Scientific Research for Priority Areas from the Ministry of Education, Culture, Sports, Science, Technology (19060009 to H.F., 20061004 and 19060016); and a Program of Basic Research Activities for Innovative Biosciences from Bio-oriented Technology Research Advancement Institution.

Competing interests statement

The authors declare no competing financial interests.

Supplementary material

Supplementary material for this article is available at
http://dev.biologists.org/lookup/suppl/doi:10.1242/dev.048199/-/DC1

References

Bleckmann, A., Weidtkamp-Peters, S., Seidel, C. and Simon, R. (2010). Stem cell signaling in Arabidopsis requires CRN to localize CLV2 to the plasma membrane. *Plant Physiol.* **152**, 166-176.

Brand, U., Fletcher, J. C., Hobe, M., Meyerowitz, E. M. and Simon, R. (2000). Dependence of stem cell fate in Arabidopsis on a feedback loop regulated by CLV3 activity. *Science* **289**, 617-619.

Casamitjana-Martínez, E., Hofhuis, H. F., Xu, J., Liu, C. M., Heidstra, R. and Scheres, B. (2003). Root-specific *CLE19* overexpression and the *sol1/2* suppressors implicate a CLV-like pathway in the control of *Arabidopsis* root meristem maintenance. *Curr. Biol.* **13**, 1435-1441.

Chinchilla, D., Zipfel, C., Robatzek, S., Kemmerling, B., Nurnberger, T., Jones, J. D., Felix, G. and Boller, T. (2007). A flagellin-induced complex of the receptor FLS2 and BAK1 initiates plant defence. *Nature* **448**, 497-500.

Clark, S. E., Running, M. P. and Meyerowitz, E. M. (1993). *CLAVATA1*, a regulator of meristem and flower development in *Arabidopsis*. *Development* **119**, 397-418.

Clark, S. E., Running, M. P. and Meyerowitz, E. M. (1995). *CLAVATA3* is a specific regulator of shoot and floral meristem development affecting the same processes as *CLAVATA1*. *Development* **121**, 2057-2067.

Clough, S. J. and Bent, A. F. (1998). Floral dip: a simplified method for Agrobacterium-mediated transformation of Arabidopsis thaliana. *Plant J.* **16**, 735-743.

Dello Ioio, R., Nakamura, K., Moubayidin, L., Perilli, S., Taniguchi, M., Morita, M. T., Aoyama, T., Costantino, P. and Sabatini, S. (2008). A genetic framework for the control of cell division and differentiation in the root meristem. *Science* **322**, 1380-1384.

DeYoung, B. J. and Clark, S. E. (2008). BAM receptors regulate stem cell specification and organ development through complex interactions with CLAVATA signaling. *Genetics* **180**, 895-904.

DeYoung, B. J., Bickle, K. L., Schrage, K. J., Muskett, P., Patel, K. and Clark, S. E. (2006). The CLAVATA1-related BAM1, BAM2 and BAM3 receptor kinase-like proteins are required for meristem function in Arabidopsis. *Plant J.* **45**, 1-16.

Diévart, A., Dalal, M., Tax, F. E., Lacey, A. D., Huttly, A., Li, J. and Clark, S. E. (2003). *CLAVATA1* dominant-negative alleles reveal functional overlap between multiple receptor kinases that regulate meristem and organ development. *Plant Cell* **15**, 1198-1211.

Fiers, M., Golemiec, E., Xu, J., van der Geest, L., Heidstra, R., Stiekema, W. and Liu, C. M. (2005). The 14-amino acid CLV3, CLE19, and CLE40 peptides trigger consumption of the root meristem in Arabidopsis through a CLAVATA2-dependent pathway. *Plant Cell* **17**, 2542-2553.

Fiers, M., Golemiec, E., van der Schors, R., van der Geest, L., Li, K. W., Stiekema, W. J. and Liu, C. M. (2006). The CLAVATA3/ESR motif of CLAVATA3 is functionally independent from the nonconserved flanking sequences. *Plant Physiol.* **141**, 1284-1292.

Geldner, N., Hyman, D. L., Wang, X., Schumacher, K. and Chory, J. (2007). Endosomal signaling of plant steroid receptor kinase BRI1. *Genes Dev.* **21**, 1598-1602.

Gordon, S. P., Chickarmane, V. S., Ohno, C. and Meyerowitz, E. M. (2009). Multiple feedback loops through cytokinin signaling control stem cell number within the Arabidopsis shoot meristem. *Proc. Natl. Acad. Sci. USA* **106**, 16529-16534.

Hejatko, J., Blilou, I., Brewer, P. B., Friml, J., Scheres, B. and Benkova, E. (2006). In situ hybridization technique for mRNA detection in whole mount Arabidopsis samples. *Nat. Protoc.* **1**, 1939-1946.

Hirakawa, Y., Shinohara, H., Kondo, Y., Inoue, A., Nakanomyo, I., Ogawa, M., Sawa, S., Ohashi-Ito, K., Matsubayashi, Y. and Fukuda, H. (2008). Non-cell-autonomous control of vascular stem cell fate by a CLE peptide/receptor system. *Proc. Natl. Acad. Sci. USA* **105**, 15208-15213.

Hobe, M., Muller, R., Grunewald, M., Brand, U. and Simon, R. (2003). Loss of CLE40, a protein functionally equivalent to the stem cell restricting signal CLV3, enhances root waving in Arabidopsis. *Dev. Genes Evol.* **213**, 371-381.

Hord, C. L., Chen, C., Deyoung, B. J., Clark, S. E. and Ma, H. (2006). The BAM1/BAM2 receptor-like kinases are important regulators of Arabidopsis early anther development. *Plant Cell* **18**, 1667-1680.

Kayes, J. M. and Clark, S. E. (1998). *CLAVATA2*, a regulator of meristem and organ development in *Arabidopsis*. *Development* **125**, 3843-3851.

Kinoshita, A., Nakamura, Y., Sasaki, E., Kyozuka, J., Fukuda, H. and Sawa, S. (2007). Gain-of-function phenotypes of chemically synthetic CLAVATA3/ESR-related (CLE) peptides in Arabidopsis thaliana and Oryza sativa. *Plant Cell Physiol.* **48**, 1821-1825.

Kondo, T., Sawa, S., Kinoshita, A., Mizuno, S., Kakimoto, T., Fukuda, H. and Sakagami, Y. (2006). A plant peptide encoded by CLV3 identified by in situ MALDI-TOF MS analysis. *Science* **313**, 845-848.

Kurakawa, T., Ueda, N., Maekawa, M., Kobayashi, K., Kojima, M., Nagato, Y., Sakakibara, H. and Kyozuka, J. (2007). Direct control of shoot meristem activity by a cytokinin-activating enzyme. *Nature* **445**, 652-655.

Laux, T., Mayer, K. F., Berger, J. and Jurgens, G. (1996). The WUSCHEL gene is required for shoot and floral meristem integrity in Arabidopsis. *Development* **122**, 87-96.

Leibfried, A., To, J. P., Busch, W., Stehling, S., Kehle, A., Demar, M., Kieber, J. J. and Lohmann, J. U. (2005). WUSCHEL controls meristem function by direct regulation of cytokinin-inducible response regulators. *Nature* **438**, 1172-1175.

Mayer, K. F., Schoof, H., Haecker, A., Lenhard, M., Jurgens, G. and Laux, T. (1998). Role of WUSCHEL in regulating stem cell fate in the Arabidopsis shoot meristem. *Cell* **95**, 805-815.

Miwa, H., Betsuyaku, S., Iwamoto, K., Kinoshita, A., Fukuda, H. and Sawa, S. (2008). The receptor-like kinase SOL2 mediates CLE signaling in Arabidopsis. *Plant Cell Physiol.* **49**, 1752-1757.

Miwa, H., Kinoshita, A., Fukuda, H. and Sawa, S. (2009a). Plant meristems: CLAVATA3/ESR-related signaling in the shoot apical meristem and the root apical meristem. *J. Plant Res.* **122**, 31-39.

Miwa, H., Tamaki, T., Fukuda, H. and Sawa, S. (2009b). Evolution of CLE signaling. *Plant Signal. Behav.* **4**, 477-481.

Mizuno, S., Osakabe, Y., Maruyama, K., Ito, T., Osakabe, K., Sato, T., Shinozaki, K. and Yamaguchi-Shinozaki, K. (2007). Receptor-like protein kinase 2 (RPK 2) is a novel factor controlling anther development in *Arabidopsis thaliana*. *Plant J.* **50**, 751-766.

Müller, R., Bleckmann, A. and Simon, R. (2008). The receptor kinase CORYNE of Arabidopsis transmits the stem cell-limiting signal CLAVATA3 independently of CLAVATA1. *Plant Cell* **20**, 934-946.

Ni, J. and Clark, S. E. (2006). Evidence for functional conservation, sufficiency, and proteolytic processing of the CLAVATA3 CLE domain. *Plant Physiol.* **140**, 726-733.

Nodine, M. D., Yadegari, R. and Tax, F. E. (2007). *RPK1* and *TOAD2* are two receptor-like kinases redundantly required for *Arabidopsis* embryonic pattern formation. *Dev. Cell* **12**, 943-956.

Ogawa, M., Shinohara, H., Sakagami, Y. and Matsubayashi, Y. (2008). Arabidopsis CLV3 peptide directly binds CLV1 ectodomain. *Science* **319**, 294.

Ohyama, K., Shinohara, H., Ogawa-Ohnishi, M. and Matsubayashi, Y. (2009). A glycopeptide regulating stem cell fate in Arabidopsis thaliana. *Nat. Chem. Biol.* **5**, 578-580.

Robatzek, S., Chinchilla, D. and Boller, T. (2006). Ligand-induced endocytosis of the pattern recognition receptor FLS2 in Arabidopsis. *Genes Dev.* **20**, 537-542.

Ruzicka, K., Simaskova, M., Duclercq, J., Petrasek, J., Zazimalova, E., Simon, S., Friml, J., Van Montagu, M. C. and Benkova, E. (2009). Cytokinin regulates root meristem activity via modulation of the polar auxin transport. *Proc. Natl. Acad. Sci. USA* **106**, 4284-4289.

Sawa, S., Demura, T., Horiguchi, G., Kubo, M. and Fukuda, H. (2005). The *ATE* genes are responsible for repression of transdifferentiation into xylem cells in Arabidopsis. *Plant Physiol.* **137**, 141-148.

Sawa, S., Kinoshita, A., Nakanomyo, I. and Fukuda, H. (2006). CLV3/ESR-related (CLE) peptides as intercellular signaling molecules in plants. *Chem. Rec.* **6**, 303-310.

Sawa, S., Kinoshita, A., Betsuyaku, S. and Fukuda, H. (2008). A large family of genes that share homology with CLE domain in Arabidopsis and rice. *Plant Signal. Behav.* **3**, 337-339.

Schoof, H., Lenhard, M., Haecker, A., Mayer, K. F., Jurgens, G. and Laux, T. (2000). The stem cell population of Arabidopsis shoot meristems in maintained by a regulatory loop between the CLAVATA and WUSCHEL genes. *Cell* **100**, 635-644.

Sharma, V. K., Ramirez, J. and Fletcher, J. C. (2003). The Arabidopsis CLV3-like (CLE) genes are expressed in diverse tissues and encode secreted proteins. *Plant Mol. Biol.* **51**, 415-425.

Shiu, S. H. and Bleecker, A. B. (2001). Receptor-like kinases from Arabidopsis form a monophyletic gene family related to animal receptor kinases. *Proc. Natl. Acad. Sci. USA* **98**, 10763-10768.

Stahl, Y. and Simon, R. (2009). Is the Arabidopsis root niche protected by sequestration of the CLE40 signal by its putative receptor ACR4? *Plant Signal. Behav.* **4**, 634-635.

Takano, J., Miwa, K., Yuan, L., von Wiren, N. and Fujiwara, T. (2005). Endocytosis and degradation of BOR1, a boron transporter of Arabidopsis thaliana, regulated by boron availability. *Proc. Natl. Acad. Sci. USA* **102**, 12276-12281.

Tucker, M. R. and Laux, T. (2007). Connecting the paths in plant stem cell regulation. *Trends Cell. Biol.* **17**, 403-410.

Voinnet, O., Rivas, S., Mestre, P. and Baulcombe, D. (2003). An enhanced transient expression system in plants based on suppression of gene silencing by the p19 protein of tomato bushy stunt virus. *Plant J.* **33**, 949-956.

Yadav, R. K., Girke, T., Pasala, S., Xie, M. and Reddy, G. V. (2009). Gene expression map of the Arabidopsis shoot apical meristem stem cell niche. *Proc. Natl. Acad. Sci. USA* **106**, 4941-4946.

Zhu, Y., Wang, Y., Li, R., Song, X., Wang, Q., Huang, S., Jin, J. B., Liu, C. M. and Lin, J. (2009). Analysis of interactions among the CLAVATA3 receptors reveals a direct interaction between CLAVATA2 and CORYNE in Arabidopsis. *Plant J.* **61**, 223-233.